ELSEVIER

Robotics and Autonomous System 17 (1996) 217–233

Robotics and Autonomous Systems

Comparison of contact sensor localization abilities during manipulation

Jae S. Son [a,*], Mark R. Cutkosky [b], Robert D. Howe [a]

[a] *Harvard University, Division of Applied Sciences, Pierce Hall, Cambridge, MA 02138, USA*

[b] *Stanford University, Department of Mechanical Engineering, Terman Engineering Center, Stanford, CA 94305, USA*

Received 1 May 1995; revised 11 July 1995

Abstract

This paper presents an experimental comparison of tactile array versus force–torque sensing for localizing contact during manipulation. The manipulation tasks involved rotating objects and translating objects using a planar two fingered manipulator. A pin and a box were selected as limiting cases of point and line contact against a cylindrical robot finger tip. Practical implementations of the two sensor types are compared theoretically and experimentally, and three different localization algorithms for the tactile array sensor are considered. Force–torque contact sensing results suffered from difficulties in calibration, transient forces, and low grasp force. Tactile array sensing was immune to these problems and the effect of shear loading was only noticeable for a simple centroid algorithm. The results show that with care, both of these sensing schemes can determine the contact location within a millimeter during real manipulation tasks.

1. Introduction

Although many researchers have studied tactile sensing devices, little work has appeared on using tactile information for manipulation. Tactile information is particularly important in manipulation by multifingered robot hands. In this context, as with human hands, rolling and sliding of the object between the fingers promises to greatly increase the mobility of the object and the dexterity of the hand.

One of the most important parameters to sense for dexterous manipulation is the location of the contact between the object and the robot finger tip. Theoretical work on grasping and manipulation shows that contact location affects many aspects of manipulation, particularly in determining grasp stability and in mapping between finger and object motions and forces (e.g. [14,21,8,15]). A number of studies have analyzed how contact locations change as objects pivot and slide against finger tips [7,12,13,17]. However, many of the factors influencing contact location cannot be predicted in unstructured environments; these factors include

* Corresponding author. E-mail: jae@hrl.harvard.edu.

SSDI 0921-8890(95)00068-2

detailed object geometry, external object forces, friction, and compliance. This implies that real-time sensing of the contact location is required.

Two methods of sensing contact location have received significant attention in robotics research literature: tactile array "extrinsic" sensing, and force–torque based "intrinsic" contact sensing. The first method uses a tactile array sensor to measure local pressure or displacement across the finger tip. Many transducer technologies have been proposed for this purpose; see [10] for a recent review. Only a few studies have appeared on the use of array information in real time control. Notable examples include [1,22], the authors contact location information from an array sensor to track object features, and Maekawa et al. [16], who used contact location sensing to prevent unwanted object rolling during manipulation.

These studies demonstrate that array sensors can localize contacts. However, the precision and generality of the algorithms for extracting location from the sensor data are far from clear. Such algorithms are often chosen ad hoc for a particular application; for example, Berger and Khosla used a simple peak-finding technique to determine the contact location. At the other extreme, Fearing [9] and Nicolson and Fearing [19] have developed elaborate algorithms based on solid mechanics analysis to localize contact with known objects with remarkable accuracy (e.g., 0.03 mm). However, this technique is relatively slow, and experimental testing was based on data acquired under static laboratory conditions where noise levels are low and the mechanical perturbations of manipulation are absent.

The other method for determining contact location is based on a completely different sensing scheme. It uses a multi-axis force–torque sensor located near the finger tip. When the force and torque measurements are combined with known shape of the finger tip, the contact location can be calculated. (A detailed exposition of this technique is provided below.) This method was originally proposed by Salisbury [20,21] and further developed by Bicchi et al. [2,5]. The name "intrinsic contact sensing" (ICS) has been proposed to distinguish this approach from tactile array "extrinsic" sensing. ICS represents a fast and potentially advantageous method of determining contact location, particularly since force–torque sensors are useful for many other perceptual and control purposes. While these schemes have been implemented for robotic exploration of object shape and mechanical properties [6,23], the use of this sensing modality in realistic manipulation tasks has not been investigated. As with tactile array sensing, there is little understanding of nonideal effects on performance.

In this paper we compare the ability of these disparate sensing modalities to determine contact location during manipulation. We consider simple signal processing algorithms that are easily executed in real time, and include the effects of noise, vibrations, and other disturbances which are inevitably present in real task execution. Our goal is not to conduct a definitive study of the absolute accuracy of these sensors, but to provide practical guidelines for immediate use in experiments. This will facilitate the use of tactile sensing and help to improve dexterous manipulation in real experiments.

We begin with a description of tactile array and intrinsic contact sensing, and analyze the main sources of error for each sensing technique. Next, we present results from experiments in which a robot finger tip containing both tactile array and force–torque sensors perform simple manipulation tasks involving changing contact forces and contact locations. For this initial study we restrict attention to planar tasks, although the results are immediately applicable to the three-dimensional case. Finally, we discuss the results and their implications for practical implementation. The results of this comparison help delineate the ways in which each type of sensor can contribute to improving robotic dexterity.

2. Tactile array sensing

2.1. Description

Tactile array sensors measure the distribution of pressure across the finger tip. This signal can be processed to provide a great deal of information about the hand–object system. Among the para-

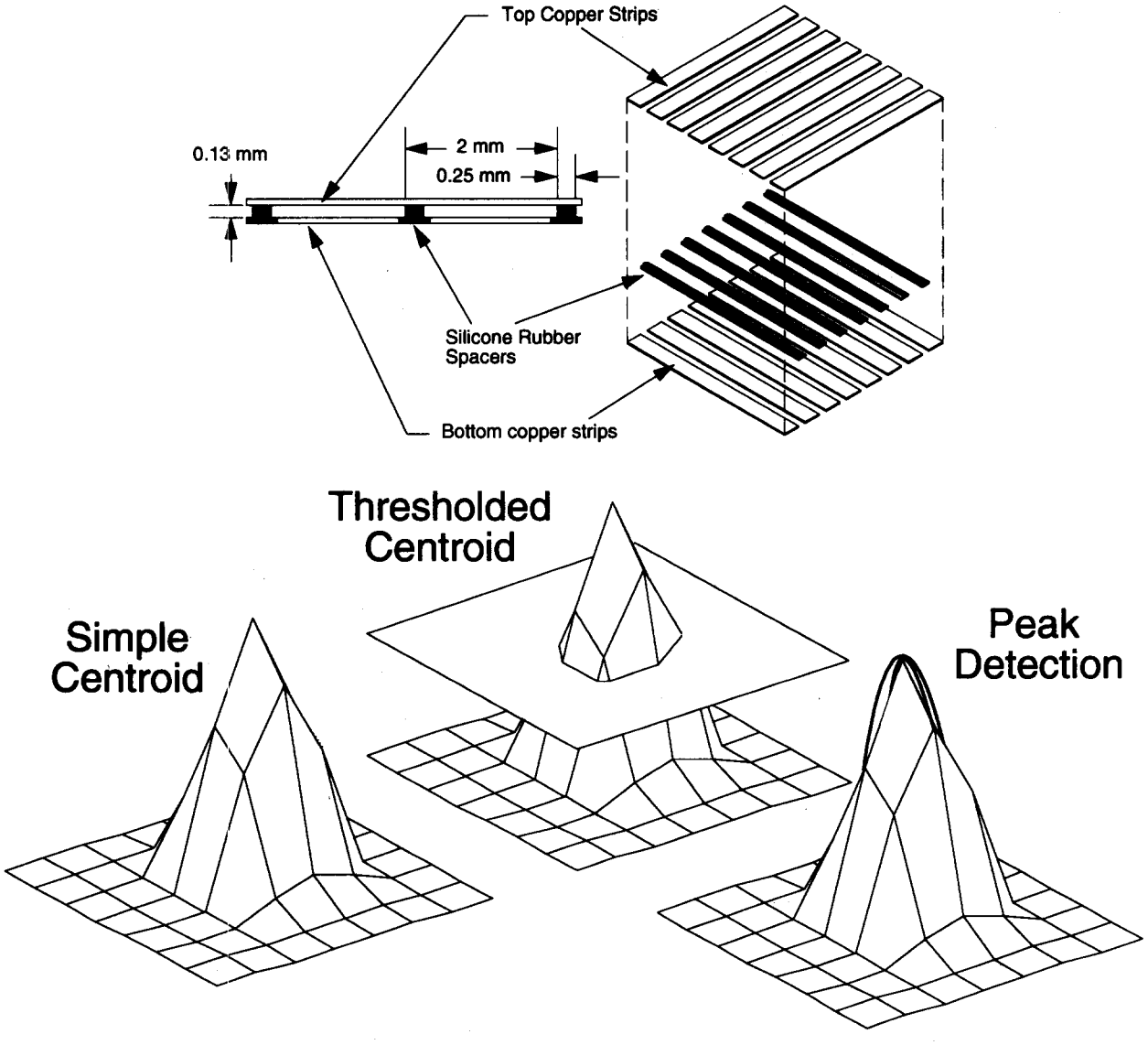

Fig. 1(a). Tactile array sensor. Left: side view; contact occurs on upper surface, compressing silicone rubber and forcing top and bottom copper strips closer together. Right: exploded view showing sensor construction. (b) Three algorithms used for determining the contact location for the array sensor. The simple centroid scheme determined the pressure centroid using all the elements of the array sensor. The threshold centroid algorithm only used tactile elements whose value was larger than 50% of the maximum tactile value to calculate the centroid. The peak detection used a quadratic fit about the maximum pressure element for each direction along the elements.

meters that can be extracted are contact location, object shape, and effective width of the pressure distribution (which determines resistance to rotational sliding [3,12]). This study focuses on the sensor's ability to localize contacts; several sensors have been developed that directly measure the effective center of the pressure distribution [18,16], but these sensors cannot be used to determine the other parameters listed above.

Tactile array sensors usually consist of a regular pattern of sensing elements. A vast number of tactile array sensing devices have been developed, although only a few have gone beyond bench-top testing [10]. The experiments reported here use a

capacitive tactile array sensor, based on an earlier design by Fearing [9]. This sensor has the advantage of simple construction and well characterized, essentially linear response. As shown in Fig. 1(a), the sensor is composed of two crossed layers of copper strips separated by strips of thin silicone rubber. As force is applied to the surface, the distance between the strips decreases, which causes the capacitance between the strips to increase. By measuring the capacitance at each crossing point, the spatial distribution of pressure across the sensor can be determined.

The sensitivity of each sensor element to a point probe is approximately 0.1 g.[1] The sensor has eight strips of 2 mm spacing in each direction, providing 64 force sensitive elements. The sensor forms a thin, compliant layer which can be easily attached to a variety of finger tip shapes and sizes. By encapsulating the sensor in a layer of elastomer, a range of surface compliance and sensitivities can be obtained. For these experiments, the 0.6 mm thick sensor is wrapped around a semi-cylindrical finger tip 25.4 mm in diameter, and covered by a 2.4 mm thick coating of silicone rubber with a modulus of $7\times10^5\,\mathrm{N/m^2}$. In contrast to soft rubber, this relatively hard rubber coating minimizes creep and viscoelastic effects that can seriously degrade dynamic response. Special-purpose electronics scan the array to measure the capacitance at each element, and the resulting pressure distribution signal for the entire array is sampled by a computer at 30 Hz.

The array sensor is calibrated by applying a uniform pressure to the surface with compressed air. First, the sensor output is measured at atmospheric pressure to obtain baseline voltages. The baseline signals for the elements are not uniform due to capacitance variations within the sensor and the cables. The sensor is then placed in a compression chamber and the pressure is increased. The array sensor output voltages are measured while the air pressure is measured with a separate pressure gauge. This calibration procedure is possible since the separation between the copper strips is mostly air and that cavity is completely sealed by the outer layer of rubber. Thus, the gain of the ijth element is

$$G_{ij} = \frac{p}{\left(V_{ij}^{p} - V_{ij}^{\text{baseline}}\right)}, \tag{2.1}$$

where V_{ij}^{baseline} is the baseline voltage and V_{ij}^{p} is the voltage measured at applied pressure p. Several different pressure settings were used to verify that the gain matrix multiplied by the output voltages resulted in a uniform response.

2.2. Contact localization algorithms

Our goal is to examine the sensor's ability to quickly determine the contact location of an object. For these experiments we consider three simple algorithms that are easily implemented and executed in real time. Therefore, centroid and peak detection schemes were selected as shown in Fig. 1(b). We assume only one point contact since the finger tip is cylindrical. The first scheme is a straightforward method of describing the contact location by the center of pressure, or centroid, as described by

$$x_{\text{centroid}} = \frac{\sum_{i=1}^{m}\sum_{j=1}^{n} x_{ij}\delta p_{ij}}{\sum_{i=1}^{m}\sum_{j=1}^{n}\delta p_{ij}},$$

$$y_{\text{centroid}} = \frac{\sum_{i=1}^{m}\sum_{j=1}^{n} y_{ij}\delta p_{ij}}{\sum_{i=1}^{m}\sum_{j=1}^{n}\delta p_{ij}}. \tag{2.2}$$

For an $m\times n$ array, the ijth tactile element position is given by x_{ij} and y_{ij}, and the pressure at that element is given by δp_{ij}. The second localization scheme aims to lessen sensitivity to low level noise on elements that are not near to the contact area by calculating the centroid with a threshold. In this case, only those elements whose values were larger than 50% of the maximum element value, were included in the summation of Eq. (2.2).

Finally, the third localization scheme interpolates the peak strain location. For point contacts, Fearing [9] used a sinusoidal curve fitted to the entire array and a gradient search method for determining peak strains, and obtained localization accuracy of 0.01 times the tactile element spacing.

[1] Array sensor response is a function of the details of the applied force distribution; see Fearing [9].

To facilitate real time computation in these experiments, a quadratic curve was fitted to three points around the tactile element with the maximum strain. From the quadratic equation, the peak strain can be interpolated with much greater precision than the tactile element spacing.

Analysis suggests that the constraining limit in determining contact location may be the presence of shear forces at contact. Previous work has shown that the response of this type of sensor is predicted with reasonable accuracy by a solid mechanics model [9,11]. Here the finger tip is treated as a linear elastic half-space, and each sensor element output provides a normal strain measurement in the vertical direction at the appropriate surface location and depth. This analysis suggests that all three of the localization schemes will be adversely affected by shear forces (i.e., the component of the contact force applied tangential to the surface of the sensor). Although it is possible to separate the even and odd components of the sensor response to better localize contact, this scheme requires that the object shape at the point of contact be symmetric with respect to the array sensor surface normal [9], so the separation algorithm cannot be applied to comprehensive object shapes.

However, measurement of our sensor response to shear forces shows that shear sensitivity is less than predicted by the model (Fig. 2). When the force vector is purely normal to the sensor surface, there is good agreement between the model and the measured response. When the force is inclined at 30°, the model predicts that the peak strain moves about 1 mm in the direction of the shear force, whereas the measured response remains centered essentially at the same location. This effect is more pronounced when the shear force is acting along the top copper strips rather than perpendicular to it.

This discrepancy is due to the sensor construction, which is more appropriately modeled by a thin beam comprised of copper strips and a relatively hard rubber outer layer supported by strips of RTV in between the tactile elements. The air gap between the copper strips decreases the effective Poisson's ratio, and the copper strips distribute shear forces further away from the point of contact. The ramification of our sensor construction is that small but significant measurements are found many cells away from the contact location. Since many tactile array sensors have continuous strips of relatively rigid materials joining the elements, this characteristic will be

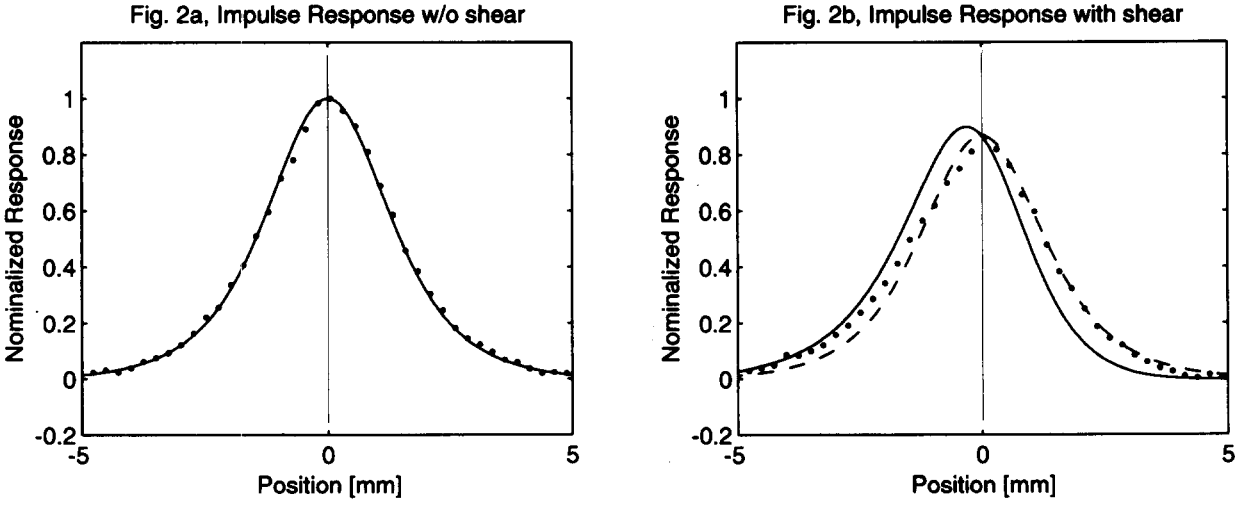

Fig. 2. (a) Impulse response without shear. Measured and theoretical impulse response of the tactile array sensor. The skin thickness and Poisson's ratio used were 2.4 mm and 0.12 mm respectively. (b) Impulse response with shear. The applied forces were 30° from the surface normal. The solid line corresponds to the expected strain based on a linear elastic model, and the broken line corresponds to strain due to the normal component response shows that the sensor is relatively to shear forces.

inherent in other types of sensors. Consequently, using a threshold is desirable when computing contact centroids. However, minimal shear sensitivity is a benefit for localizing contact since the errors generated by shear forces are significantly reduced.

The three localized schemes represent specific points along a continuum. The centroid scheme takes the whole array into consideration, while the peak localization scheme focuses on just a few elements. The threshold centroid scheme is a compromise where only certain elements meeting the criteria are taken into consideration. The peak localization scheme will be less stable than the centroid methods. For example, without contact the peak localization scheme can jump all over the sensor area, but the averaging effect for the centroid scheme provides a more stable output.

3. Intrinsic contact sensing

3.1. Analysis

Intrinsic contact sensing (ICS) combines finger tip force–torque sensing with a model of the finger tip shape to estimate contact location. The principle of operation is more easily understood if we assume that the object contacts the finger tip at a single point with no torques transmitted at the contact. Then the torque measured by the sensor is caused exclusively by the measured force at the contact location. The combination of forces and torque determines a line of action, and the intersection of this line of action with the finger tip surface is the point at which the contact occurs.

Although the ICS algorithm as developed by Salisbury [20] and Bicchi et al. [5] is fully three dimensional, we restrict our experiments to the planar case. Since the manipulator operates in the plane and the cylindrical finger tip is oriented to form a circular cross section in the plane, the origin of the coordinate frame was located at the center of the finger tip (Fig. 3). The force–torque relation is

$$\boldsymbol{m} = \boldsymbol{r} \times \boldsymbol{f}, \tag{3.1}$$

where $\boldsymbol{m}$ is the three-element measured torque vector, $\boldsymbol{f}$ is the three-element force vector, and $\boldsymbol{r}$ is the three-element vector from the origin to the point of contact. In the planar case there are only two force components and one torque component, so this reduces to

$$m = f_y x - f_x y, \tag{3.2}$$

where m is the moment perpendicular to the plane, f_x, f_y are the planar force components, and x, y are the contact coordinates in the plane. The finger tip

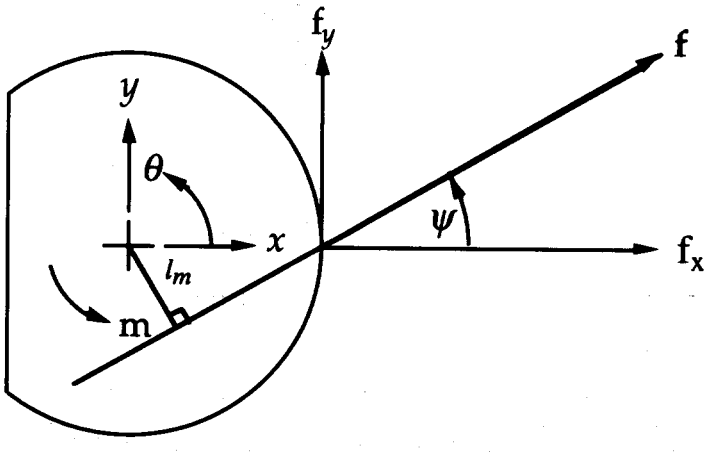

Fig. 3. Finger tip cross section showing coordinates and variables used in the ICS calculations.

shape is described by

$$r^2 = x^2 + y^2, \tag{3.3}$$

where r is the radius of the finger tip. Because the line of action will intersect the finger tip at two points, we must specify that $x > 0$ to ensure that we find the correct point.

Polar coordinates were used for the experiment since this permits specification of the contact location in terms of one parameter, θ, as r constant. The distance along the finger circumference, measured from the x-axis, is then simply $r\theta$.

The force vector orientation can be determined easily by the ratio of f_y over f_x. By extending the force vector line of action, the lever arm for the moment about the origin, l_m, can be determined. Thus,

$$m = fl_m = fr\sin(\psi - \theta), \tag{3.4}$$

where $f = \sqrt{f_x^2 + f_y^2}$ is the force magnitude and ψ is the force vector angle. Solving for θ we obtain

$$\theta = \tan^{-1}\left(\frac{f_y}{f_x}\right) - \sin^{-1}\left(\frac{m}{fr}\right). \tag{3.5}$$

This equation imposes a condition that $|m/(fr)| < 1$. This requirement simply limits the maximum moment generated through the finger radius, which means that the force sensor values must be checked before applying this ICS algorithm.

To understand the limits of this scheme, we look briefly at the theoretical limits to localization accuracy. Using Eq. (3.5), we can take the partial derivative with respect to each parameter and multiply it by the parameter estimation error to obtain an estimate of the noise sensitivity. Since we have two forces, one torque, and a radius in the estimation formula, the maximum estimation error is

$$\begin{aligned}
\delta\theta_{\max} &= f(f_x, f_y, m, r) \\
&= \left[\left(\frac{\partial\theta}{\partial f_x}\Delta f_x\right)^2 + \left(\frac{\partial\theta}{\partial f_y}\Delta f_y\right)^2 + \left(\frac{\partial\theta}{\partial m}\Delta m\right)^2 + \left(\frac{\partial\theta}{\partial r}\Delta r\right)^2\right]^{1/2} \\
&= \left[\left(\frac{mf_x\Delta f_x}{rf^3\sqrt{1-(m/fr)^2}} - \frac{f_y\Delta f_y}{f_2}\right)^2 + \left(\frac{mf_y\Delta f_y}{rf^3\sqrt{1-(m/fr)^2}} - \frac{f_x\Delta f_y}{f^2}\right)^2 + \frac{\Delta m^2}{fr(fr-m)} + \frac{m^2\Delta r^2}{f^2r^4(1-(m/fr))}\right]^{1/2}.
\end{aligned} \tag{3.6}$$

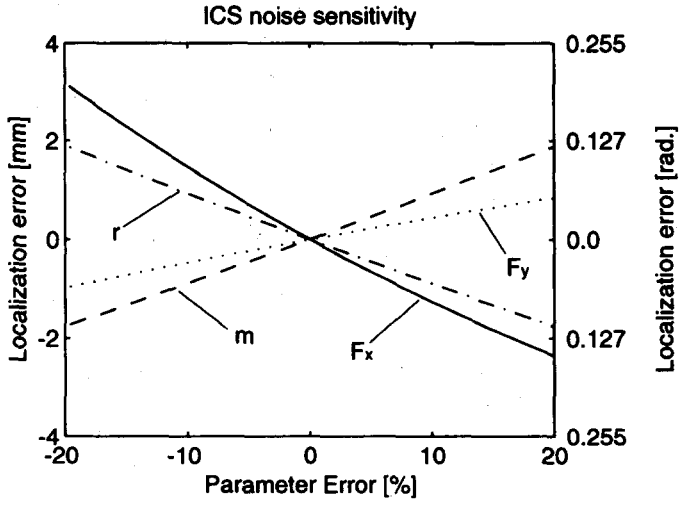

Fig. 4. The expected localization errors based on parameter variations are shown for forces, moment and finger tip radius. Within ±20% variation, the localization errors are approximately linear.

Fig. 4 shows the estimation error along the cylindrical surface as a function of each parameter. The parameters are varied ±20% of the nominal values for the contact condition shown in Fig. 3, for the case of contact location $\theta = 0$ and force orientation $\psi = 30°$. We observe that within this range, contact location varies almost linearly with small errors in f_x, f_y, m and r. Similar results are obtained for other contact locations and force orientations. The predicted total errors are on the order of a few millimeters, which correlates well with the experimental results presented below.

The foregoing analysis treats the contact as a single point with no transmitted torques. For compliant surface contacts, it can be shown that intrinsic contact sensing determines the contact centroid or center of pressure as an estimate of the contact location [5]. The measured force acting on a contact centroid is equivalent to the distributed pressure over the contact area. This analysis represents the simplest of three algorithms presented by Bicchi et al. [5]. The other methods attempt to compensate for the use of compliant finger tips in three dimensions, where contact torques about the surface normal may be generated. In the planar experiments presented here, these contact torques are not pertinent.

3.2. Calibration

Multi-axis force–torque sensors typically use a set of coupled single-component strain gauges to make the force and torque measurements. The relationship between the measured strains and the actual forces and torques can be expressed as a linear transformation

$$F = CV, \tag{3.7}$$

where $F = [f_x\, f_y\, m]^T$ and V is the measured strain voltages. The C matrix must be obtained through calibration, and this procedure requires applying controlled forces on multiple locations on the finger tip surface at various orientations. By recording the strain gauge voltages and calculating the moment generated at the finger tip center by the applied forces, a least squares fit calibration matrix can be obtained.

In these experiments, the three-axis sensor is a U-shaped aluminum structure with semiconductor strain gauges mounted at three locations. Despite care in the calibration process, the calibration matrix was not very well-conditioned, very small errors in the measured voltages could produce significant errors in the calculated force components. A major source of this was due to the compliant finger tips. Because a pointed indenter was used to apply the desired forces on the finger tip, the accuracy of the calculated moment was reduced by the uncertainty in contact location due to skin deformation. The finger tip deformation also generated unmodeled shear forces which reduced the accuracy of the applied force. Bicchi and Canepa [4] provide a thorough discussion of the calibration process and the issues associated with it. The calibration matrix used in these experiments is

$$C = \begin{bmatrix} -126 & -51 & 127 \\ 378 & -6 & -72 \\ 396 & -128 & 22 \end{bmatrix}.$$

Because the force sensor was designed for planar applications with forces only in the manipulation plane, it showed slight cross-sensitivity to out-of-plane forces. The experiments were conducted in the horizontal plane, so the weight of the grasped object resulted in a constant offset of a few millimeters in the ICS localization results. This offset was subtracted from the results presented in Section 4.

4. Experiments

4.1. Experimental apparatus

A simple two-fingered planar hand was used to conduct these manipulation experiments. Each finger has two degrees of freedom in the horizontal plane, with direct drive motors and a five bar linkage, as seen in Fig. 5. The servo rate was set to 300 Hz and object stiffness control was used to command the desired object location and orienta-

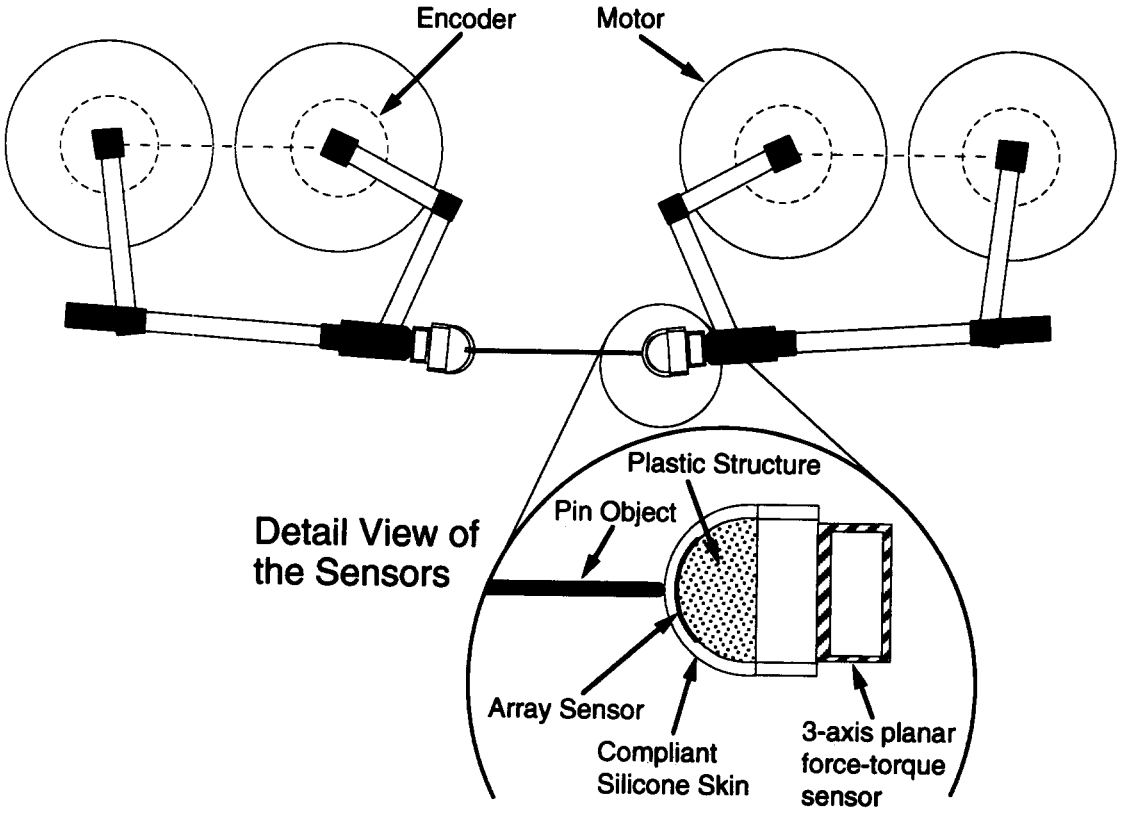

Fig. 5. Schematic of the manipulator during the pin manipulation experiment. A tactile array sensor and a force sensor are mounted on the right fingertip.

tion within the workspace [21]. Both finger tips were mounted on the three-axis force sensors described above, and the right finger tip with the tactile array sensor weighed 35 g, with an outer radius of 15.7 mm.

4.2. *Procedures*

To investigate contact localization during manipulation, two objects and two manipulation tasks were chosen. A 10 cm long pin with spherical ends and a 1.6 mm radius tip, and a 10 cm wide square box were used as the objects. The pin and the box weighed 4.2 and 77 g, respectively. The two manipulation tasks involved rotating the object $\pm 20°$ about the center of the object, and moving the object in a 2 cm×2 cm square trajectory at a relatively high velocity of 4 cm/s.

These particular objects and tasks were selected to include many of the conditions that might be encountered in general dexterous manipulation tasks. In particular, the tasks generate significant shear forces and accelerations. When rotating the pin, the force angle with respect to the finger changes. This generates shear forces at the contact location which may reduce the localization ability of the array sensor. On the other hand, intrinsic contact sensing measures shear forces and uses this information to localize contact so variations in shear forces are taken into consideration. Since the object is a pin and the contact location remains essentially constant, the actual localization plot as a function of time should be a horizontal line. To measure the ability to track changes in contact location, the pin was replaced with a box having the same dimensions in length. As the object rotates, the finger tip rolls on the object and the

expected trace for contact localization is approximately a triangular wave form as a function of time.

The next task of translating the object was designed to test the ICS scheme. At the corners of the square trajectory, the grasped object and the finger tips experience high accelerations, so the mass of the object and the finger tips will generate inertial forces to which the force sensor will respond. These forces will appear as interference on the force sensor signal, but the tactile array sensor, with its low mass and distributed sensing elements, should not respond. We wanted to observe the effects of these accelerational forces on the ICS algorithm and to verify that the array sensor is immune to them. When translating the box, the finger tip must roll slightly against the box to obtain the desired trajectory, while the expected localization trace for the pin is a horizontal line as a function of time.

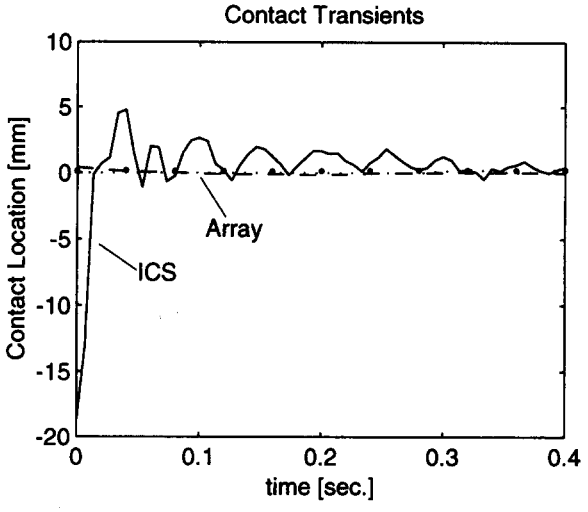

Fig. 6. Comparison of transient responses of instrinsic and array sensing schemes. Large negative spike in ICS is due to low force levels at initial contact

4.3. Results

In Figs. 6–10, typical localization results for intrinsic contact sensing and the three localization schemes for the array sensor are plotted. For all the array sensor plots, the heavy solid dots are the peak localization algorithm, the dashed lines are the simple centroid algorithm, and the dotted lines are the thresholded centroid algorithm. The coordinate origin for contact localization is set at the location corresponding to $\theta=0$ and the distance is along the circumference of the finger tip.

We begin by comparing tactile array and ICS localization at the instant of contact. Manipulator fingers were positioned close to the object and the controller commanded a feed forward grasp force to grasp the object, and data acquisition started immediately. The feed forward grasp force of 3 N was used to generate the desired grasp force on the object. Initial impact on the object caused a force spike of approximately 1 N in magnitude. This along with the zero contact force before contact explains the large localization error associated with the intrinsic contact sensing scheme at the instant of contact as shown in Fig. 6. The array sensor is insensitive to this contact transient.

4.3.1. Pin manipulation experiments

Results from translating the pin in a square trajectory are shown in Fig. 7(a)–(d). In Figs. 7(a) and (b), the pin is located at the center of the fingertip and shear forces were negligible, while for Figs. 7(c) and (d), the contact location is shifted by approximately 3 mm and shear forces with respect to the surface normal were about 19% of normal forces. Since the object velocity was 4 cm/s and the total length of the trajectory was 8 cm, the trajectory was completed in 2 s, but it was repeated several times. The measured peak accelerations at the corners of the trajectory were between 80 and 130 cm/s^2.

For Fig. 7(a) and (b) the actual trajectory of the contact location is a horizontal line at position 0 mm, and for Fig. 7(c) and (d) the actual trajectory is a horizontal line at position −3 mm. We observe that the random noise associated with ICS is larger in comparison to the tactile array sensor. There are two reasons for this. First, the random noise level of the force sensor was higher than the array sensor. Second, the finger tip mass acts along with the force sensor to mechanically amplify any vibrations and manipulator transmission noise.

Although the contact location does not change against the finger tip, localization spikes are seen

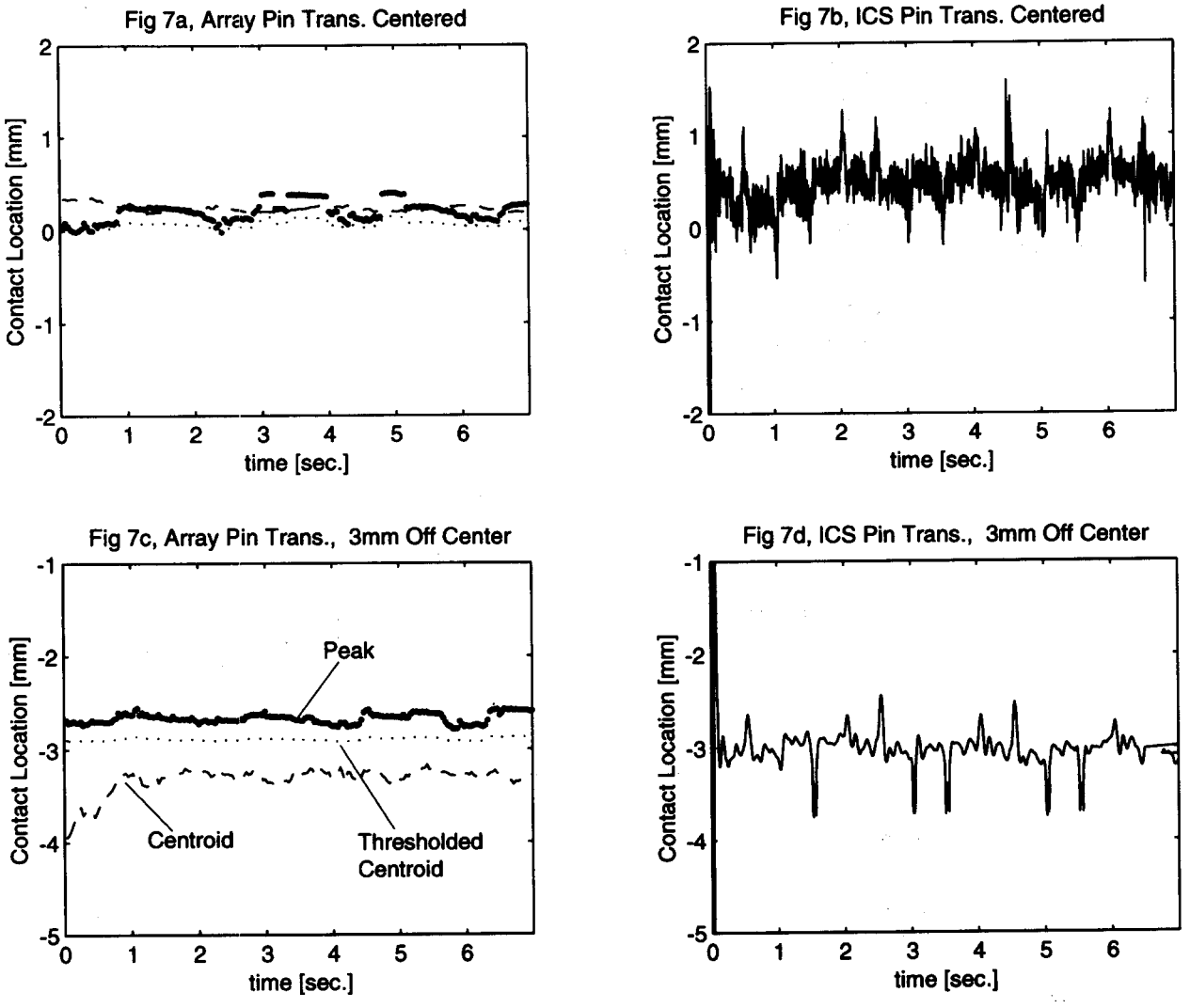

Fig. 7. Contact localization for pin translation experiment. (a),(c) Array sensor; (b),(d) ICS. (a),(b) pin centered on finger tip ($\theta = 0$, no shear forces); (c),(d) pin displaced 3 mm ($\theta = 0.19$ rad, shear force present). The diffrent appearance between the two ICS traces is a result of filtering the ICS data. A two pole low pass Butterworth filter was used with the 3 dB set to 10 Hz. Although the higher frequency noise is reduced, the transient acceleration spikes remain unaffected.

every 0.5 s in Fig. 7(b) and (d) where the trajectory goes through a corner and inertial forces are generated. A clear correlation between object accelerations and localization ability for the ICS is shown by the periodicity of the trace corresponding to object accelerations. In Fig. 7(d), the ICS data were filtered using a two-pole low pass filter with the 3 dB set to 10 Hz. The random noise associated with ICS shown in Fig. 7(b) is eliminated, but the accelerational transients remain essentially unchanged.

Fig. 7(a) shows that the array sensor is immune to accelerations, but Fig. 7(c) shows that when the contact location is shifted approximately 3 mm, shear forces influence the centroid algorithm. Since the simple centroid algorithm uses all the tactile elements of the sensor, shear force generated deflections far from the contact location are

included in the calculations, thus biasing the results.

Results from the pin rotation experiments are shown in Fig. 8(a)–(d). In Fig. 8(a)–(b), the pin is located at the center of the finger while for Fig. 8(c) and (d), the location is shifted again by 3 mm. While holding a pin and rotating it, the contact location does not change against the finger tip, but the force vector changes along with the rotation angle. Since the contact location is fixed, the actual trajectory for these plots is also a horizontal line. Shear forces generated during the pin rotation experiment reduces the tactile array sensor's ability to localize contact since shear forces create normal strains. However, this localization error is only pronounced for the simple centroid scheme at very sharp angles, as shown in Fig. 8(c).

Although the noise associated with the ICS signal has not increased, the localization trajectory is significantly different from the expected and the array sensor results. Theoretically, the ICS scheme should be insensitive to shear forces since it uses this information, but calibration difficulties result

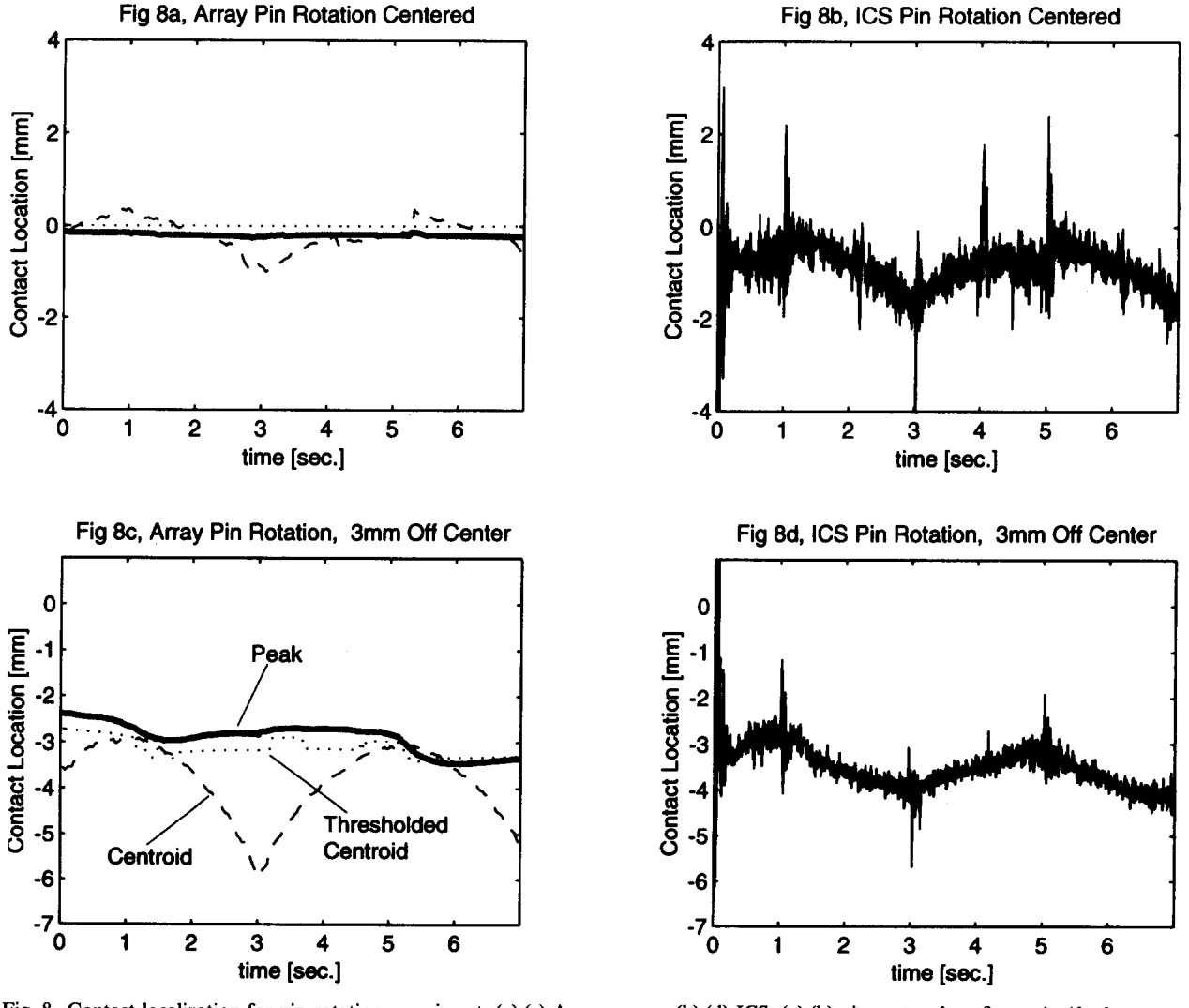

Fig. 8. Contact localization for pin rotation experiment. (a),(c) Array sensor; (b),(d) ICS. (a),(b) pin centered on finger tip ($\theta = 0$, no shear forces); (c),(d) pin displaced 3 mm ($\theta = 0.19$ rad, shear force present).

Table 1
RMS and peak localization errors for the pin rotation and translational experiments. The first three columns are the tactile array sensors and in the fourth column are the Intrinsic Contact sensor errors excepting the initial contact transient errors

	Centroid	Threshold	Peak	ICS
Pin translation centered-RMS error(mm)	0.05	0.10	0.09	0.18
Pin translation centered-Peak error(mm)	0.12	0.17	0.23	0.10
Pin rotation offcenter-RMS error(mm)	0.78	0.18	0.25	0.34
Pin rotation offcenter-Peak error(mm)	2.94	0.40	0.52	2.42

in errors, as seen by the triangular wave deviations from the actual location.

As seen in Fig. 8(b) and (d), localization error spikes are observed for ICS due to rapid acceleration when the direction of rotation changes. Additional localization spikes are seen when $\theta = 0$ for Fig. 8(b). Force transients can be generated when the object goes though $\psi = 0$ due to the sign reversal of the shear force on the compliant rubber skin.

Table 1 compares the localization errors associated with each of the sensing schemes for the pin rotation and translation experiments. Since we are interested in larger systematic errors rather than random errors associated with sensor's signal-to-noise ratio, we observe the following. First, transient peak errors for ICS are several times larger than the array sensor. Second, shear forces introduced in the pin rotation experiment only affects the centroid algorithm of the tactile array sensor. This error is most clearly seen during off centered pin rotation.

4.3.2. *Box manipulation experiments*

For plots 9 and 10, the experiments involved translating and rotating a box, similar to the pin experiments. Contact locations calculated based on the kinematics of the robot and the object are plotted as a solid line for comparison purposes. This calculation requires a priori knowledge of object properties which would not be available in unstructured environments, but represents a reasonable approximation to the actual contact location.

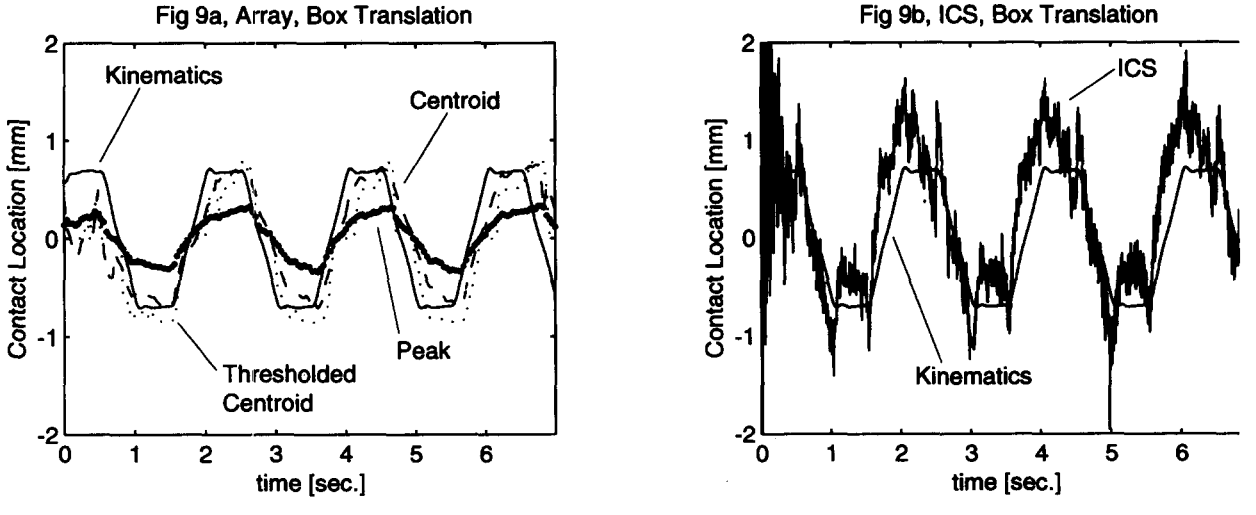

Fig. 9. Contact localization for box translation experiment. (a) Array sensor; (b) ICS. Solid line represents calculated results using robot kinematics.

The expected trace for the box translation experiment in Fig. 9(a) and (b) is a trapezoidal wave since the fingers roll mostly during the vertical traverse phase. Again, the ICS trace has more high frequency noise than the array sensor traces, even though the frequency content of the ICS data is mostly under 20 Hz, and thus comparable to the bandwidth of the array sensor signal. The peak localization scheme is significantly different from the centroid schemes. This tells us that violating our initial assumption about single point contact affects the peak localization algorithm the most.

For the case of rotating a box shown in Fig. 10(a) and (b), the contact location changes as the finger tip rolls against the box. Actual peak to peak object rotation is slightly less than 40° since the fingers roll against the object, and this effect is not taken into consideration in the controller calculations. Because of slow manipulation speed and the absence of shear forces during rolling, both sensing schemes show about the same accuracy in tracking the contact location.

Careful examination of the peak localization scheme in Fig. 10(a) reveals discontinuities in the localization trace. Ideally, the finger and the box should form a uniform line contact, but during manipulation, the peak strain jumps positions within this line of contact due to edge effects and nonuniform loading associated with manipulation. Since all the tactile elements were used for the peak detection algorithm, these effects reveal themselves as discontinuities in the trace.

4.4. *Discussion*

For many years, tactile sensing has promised to improve dexterity of robots. The goal of this paper is to examine fast, practical methods which can be implemented easily on real manipulators. From these calculations and experiments we can derive several important lessons. Both the tactile array and the ICS schemes were able to localize contact within a few millimeters in the presence of manipulation noise such as shear and inertial forces. Although the hardware for the ICS is much simpler, there are serious difficulties in the calibration procedure, especially with soft finger tips. Many of the errors associated with the intrinsic sensing method can be traced to difficulties in calibration. When calibrating a force sensor for this application, it is important to precisely control the contact locations as well as the magnitudes and orientations of the applied point load forces. In addition, it is desirable to do so with the finger tip attached. However, a point load indents the rubber finger tip, making contact

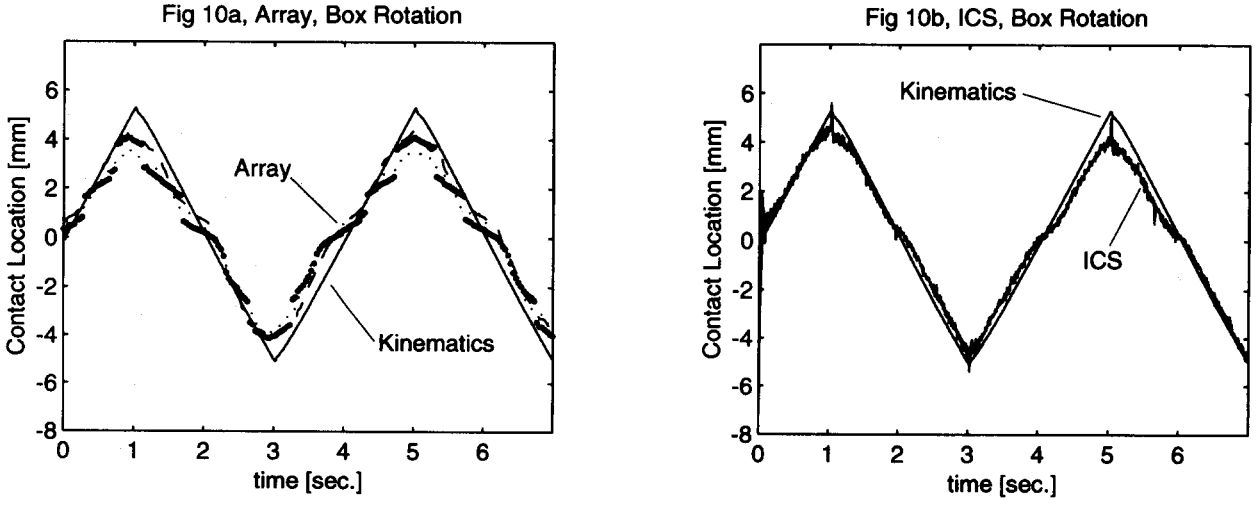

Fig. 10. Contact localization for box rotation experiment. (a) Array sensor; (b) ICS. Solid line represents calculated results using robot kinematics.

location imprecise and generating shear forces. This is a generic problem for all force sensors with compliant finger tips.

The ICS algorithm should be thresholded to obtain reliable contact location during initial contact. Before firm contact is established, the signal levels are on the order of the noise level so the localization errors are large. In addition, inertial forces can affect the ICS method, so rapid accelerations generated during manipulation should be minimized or ICS derived location should be ignored during that period. One way to reduce inertial forces is to use a smooth trajectory which minimizes accelerations. Another method involves minimizing the finger tip weight. Since the calibration is conducted on the finger tip surface, any forces generated on the surface, including object inertial forces, will be taken into consideration in the calculations. Therefore, only the inertial forces generated by the finger tip mass affect the localization scheme. This phenomena can be observed by the fact that despite an object weight ratio of 18 : 1 for the box to the pin, localization errors associated with the translation experiments remain essentially constant.

The tactile array sensor, on the other hand, is a more complex device. It requires a far greater effort to fabricate the sensor and the associated electronics. The calibration procedure required for the array sensor would have been similar, but using compressed air simplified the calibration procedure tremendously. In addition, the spatial characteristics of the sensor elements are uniform, so spatial calibration is not required. The lower mass associated with the array sensor makes it less susceptible to sudden accelerations for those elements not in contact with the object.

The three schemes for localizing contact provided interesting comparisons. The primary difference between the schemes seemed to be their sensitivity to shear forces, with the simple centroid scheme being most susceptible. For point contacts, the peak and thresholded algorithms worked well in rejecting shear induced strains. However, the centroid schemes performed better for larger contact areas. This suggests that the type of algorithm used should be tailored to the expected contact conditions.

Examination of the array sensor pressure distribution during box manipulation reveals that the pressure distribution is not uniform as expected. There are edge effects and shifting of peak locations. This creates some difficulty for the peak localization scheme which jumps from one peak to another in a discrete fashion. This suggests that for manipulating flat objects, a spherical tactile sensor or a softer rubber surface might provide more consistent information.

5. Conclusions

This paper presents calculations and measurements of localization errors in characteristic manipulation tasks using intrinsic contact sensing and tactile array sensing schemes. With the exception of ICS transients, experimental results show that the RMS localization error for all the sensing schemes are less than 1 mm. The ICS scheme, while potentially fast and accurate, requires a great deal of care in the calibration process, and it is affected by transient forces (e.g., initial contact, object accelerations) which can produce errors of several millimeters. It also suffers from a poor signal-to-noise ratio at low contact forces. Therefore, to effectively use ICS, finger tip mass should be minimized, contact forces should be thresholded before applying the algorithm, and either accelerations should be minimized or inertial transients must be taken into account.

The tactile array sensor works well for contact localization. However, it is inherently slower than ICS and much more difficult to construct and integrate with the rest of the manipulator and controller. The tactile array sensor's sensitivity to shear loads was minimal and only noticeable at very sharp angles using a simple centroid scheme. For manipulation purposes, the shear load effects can be minimized using a peak detection or a thresholded centroid algorithm. Since peak localization schemes work well for point contacts, and centroid localization schemes work better for larger

contact areas, algorithm selection should be based on manipulation object types. If this information is not available, a thresholded centroid algorithm should be a good compromise.

With care, both of these sensing schemes can provide contact localization accuracy of less than a millimeter in real manipulation tasks. This should be sufficient for a large number of application domains. Regarding the general question of which type of sensor should be used, or which sensor performs better, other benefits of each sensor should be considered as well. The force sensor has many other uses such as directly measuring contact forces and implementing stiffness controllers. The array sensor, can provide shape information as well as pressure distribution of the contact area. Naturally, both sensors can be used to provide redundant information to increase robustness of the entire system.

Acknowledgements

The authors would like to thank Marc Tremblay, Dean Chang, and Jim Hyde of Stanford University for their help with the experimental component of this work, and Ron Fearing of the University of California at Berkeley for providing the array sensor electronics design. This work was supported by the Office of Naval Research under ONR Grants No. N00014-92-J-1814 and N00014-92-J-1887. Support for the first author was provided by a Doctoral Fellowship from Hughes Space and Communications Company.

References

[1] A.D. Berger and P.K. Khosla, Using tactile data for real-time feedback, *International Journal of Robotics Research* 10(2) (1991) 88–102.

[2] A. Bicchi, Intrinsic contact sensing for soft fingers, *The Proceedings of the 1990 IEEE International Conference on Robotics and Automation*, Cincinnati, OH (1990) 968–973.

[3] A. Bicchi, M. Bergamasco, P. Dario and A. Fiorillo, Integrated tactile sensing for gripper fingers, *Proceedings of the 7th International Conference on Robot Vision and Sensory Controls*, Zurich (1988).

[4] A. Bicchi and G. Canepa, Optimal design of multivariate sensors, *Measurement Science and Technology* 5(4) (1993) 319–32.

[5] A. Bicchi, J.K. Salisbury and D.L. Brock, Contact sensing from force measurements, *International Journal of Robotics Research* 12(3) (1993) 249–262.

[6] D. Brock and S. Chiu, Environment perception of an articulated robot hand using contact sensors, *Robotics and Manufacturing Automation*, Vol. PED 15, ASME Winter Annual Meeting. Miami (1985) 89–96.

[7] A. Cole, P. Hsu and S. Sastry, Dynamic control of sliding by robot hands for regrasping, *IEEE Transactions on Robotics and Automation* 8(1) (1992) 42–52.

[8] M.R. Cutkosky and I. Kao, Computing and controlling compliance of a robotics hand, *IEEE Transactions on Robotics and Automation* 5(2) (1989) 151–165.

[9] R.S. Fearing, Tactile sensing mechanisms, *International Journal of Robotics Research* 9(3) (1990) 3–23.

[10] R.D. Howe, Tactile sensing and control of robotic manipulation, *Journal of Advanced Robotics* 8(3) (1994) 245–261.

[11] R.D. Howe and M.R. Cutkosky, Dynamic tactile sensing: perception of fine surface features with stress rate sensing, *IEEE Transactions on Robotics and Automation* 9(2) (1993) 140–151.

[12] R.D. Howe and I. Kao and M.R. Cutkosky, The sliding of robot fingers under torsion and shear loading, *Proceedings of the 1988 IEEE International Conference on Robotics and Automation*, Philadelphia (1988) 103–108.

[13] I. Kao and M.R. Cutkosky, Quasistatic manipulation with compliance and sliding, *International Journal of Robotics Research* 11(1) (1992) 20–40.

[14] J. Kerr and B. Roth, Analysis of multifingered hands, *The International Journal of Robotics Research* 4(4) (1986) 3–17.

[15] Z. Li, P. Hsu and S. Sastry, Grasping and coordinated manipulation by a multifingered robot hand, *International Journal of Robotics Research* 8(2) (1989) 33–50.

[16] H. Maekawa, K. Komoriya and K. Tanie, Manipulation of an unknown object by multifingered hands with rolling contact using tactile feedback, *Proceedings of the 1992 IEEE/RSJ International Conference on Intelligent Robots and Systems, IROS '92*, Raleigh, NC, July 7–10 (1992) 1877–1882.

[17] D.J. Montana, The kinematics of contact and grasp, *International Journal of Robotics Research* 7(3) (1988) 17–32.

[18] Y. Nakamura, H. Hanafusa and N. Ueno, A piezoelectric film sensor for robotic end-effectors, in: A. Pugh, ed., *Robot sensors, Vol. 2: Tactile and Non-Vision* (IFS Publications/Springer, Berlin, 1986) 247–57.

[19] E.J. Nicolson and R.S. Fearing, The Reliability of Curvature Estimates from Linear Elastic Tactile Sensors, *To appear in 1995 IEEE International Conference on Robotics and Automation*, Japan (1995).

[20] J.K. Salisbury, Interpreting contact geometries from force measurements, *Proceedings of the 1st International Symposium on Robotics Research*, Bretton Woods, NH (1984).

[21] J.K. Salisbury, Kinematic and force analysis of articulated hands, in: M.T. Mason and J.K. Salisbury, eds., *Robot Hands and the Mechanics of Manipulation* (MIT Press, Cambridge, MA 1985).

[22] P. Sikka, H. Zhang and S. Sutphen. Tactile servo: control of touch-driven robot motion, *Experimental Robotics III: The Third International Symposium*, Kyoto, Oct. 28–30, Lecture Notes in Control and Information Sciences, Vol. 200 (Springer, Berlin, 1993) 221–233.

[23] T. Tsujimura and T. Yabuta, Object detection by tactile sensing method employing force/torque information, *IEEE Transactions on Robotics and Automation* 5(4) (1989) 444–50.

Jae S. Son received B.S degree with honours from Michigan State University in 1990 and S.M in Engineering from Harvard University in 1993. He is presently working on his Ph.D at Harvard with full fellowship from Hughes Space and Communication Company. His thesis research focuses on utilizing tactile sensing in autonomous multi-fingered manipulation. Additional research interests are mechanical design, design methodologies, and tactile sensing applications.

Mark R. Cutkosky is the Charles M. Pigott Associate Professor and Associate Chair for Design and Manufacturing in the Mechanical Engineering Department at Stanford. He is a co-director of SIMA, the Stanford Integrated Manufacturing Association and a member of the Stanford Center for Design Research where he conducts research in dextrous manipulation with tactile sensors and in computational support for concurrent engineering. Dr. Cutkosky received his Ph.D from Carnegie-Mellon University and B.S from the University of Rochester. He joined Stanford in 1985, after working for several years in the Robotics Institute at Carnegie-Mellon University and as a design engineer at ALCOA, in Pittsburg, Pennsylvania. He is an NSF Presidential Young Investigator and Anderson Faculty Scholar at Stanford and a member of ASME, SME, Sigma XI.

Robert D. Howe received B.A. in physics from Reed College in 1979, then worked as a design engineer in the electronics industry for several years. He attended graduate school at Stanford University and received Ph.D. degree in 1990. He is presently Associate Professor of Mechanical Engineering at Harvard University. His research interests include robotic manipulation, tactile sensing and display, teleoperation, and biological motor control.